Whistling in the Clavichord

Jean-Théo Jiolat, Jean-Loïc Le Carrou, Christophe d'Alessandro

Whistling in the Clavichord

Jean-Théo Jiolat,[1] Jean-Loic Le Carrou,[1] and Christophe d'Alessandro[1]
Sorbonne Université, CNRS, Institut Jean Le Rond d'Alembert, Équipe Lutheries-Acoustique-Musique, F-75005 Paris, France

Sympathetic string vibration plays an essential role in the clavichord's sound quality and tonal identity. Sympathetic vibration comes from the undamped string segments between the bridge and tuning pins. Under some conditions, a specific note, a whistling tone, stands out of the reverberation halo due to sympathetic vibration. It is hypothesized that this whistling tone comes from resonance between played and sympathetic segments of strings that are coupled through the bridge. Vibratory measurements for three pairs of excited and sympathetic strings are conducted on a copy of a historical instrument by Hubert (1784). The influences of bridge mobility and tuning on sympathetic string frequency and damping are studied. The results show a significant increase in vibratory amplitude, frequency veering and damping increase of the string segments when tuning approaches frequency coincidence. Numerical simulations of a reduced clavichord model corresponding to the experiments are conducted using the modal Udwadia-Kalaba formulation. Simulation gives a more accurate picture of the veering phenomenon. Simulation and experimental results are in good agreement, showing that whistling in the clavichord comes from string resonance. It is favored by frequency coincidence between excited and sympathetic string segments and by higher bridge mobility.

Pages: 1–11

I. INTRODUCTION

Sympathetic string vibration plays an essential role in the clavichord's sound quality and tonal identity. Sympathetic vibration comes mainly from the segments of strings between the bridge and tuning pins that are not damped with felt in the clavichord (coined S-strings in this article). These segments vibrate freely when some energy from the played segments of the strings is transferred through the bridge motion. The played segment of a string (coined P-string) is between the tangent and the bridge. Depressing a key on the keyboard sets the P-string into vibration (see Figure 1 for the disposition of the strings in the instrument). Note that S-strings are never damped in historical instruments, contrary to contemporary instruments, e.g., square pianos because their contribution reinforces the intrinsically weak sound of the instrument.

The number of strings, then of P-string and S-string segments, is typically between 70-122 for most instruments. All the S-strings are excited when a tone is played on the keyboard because the bridge vibrates. Ancient makers of the finest instruments have meticulously adjusted sympathetic strings. As early as 1511 by Sebastian Virdung[2] mentioned *resonance* coming from the sympathetic string. Marin Mersenne[3] and Jakob Adlung[4] discussed noted the effect of the sympathetic string. The tonal consequences of S-strings and comparison with room reverberation data have been investigated in previous works[5–7]. Significant effects of sympathetic strings on the instrument's tonal quality are found. Sound duration is significantly increased, and the spectrum is enhanced; The overall contribution of all the S-strings results in a halo in the radiated sound, comparable to sound reverberation, but with specific decay patterns that does not correspond to simple room acoustic.

A specific sound effect occurs when the frequencies of an S-string partial and a P-string partial coincide. It results in a significant and audible increase in the vibratory amplitude of the S-string that reinforces the sound quality of the played tone. As a result, a noticeable whistling tone emerges and stands out of the reverberation halo. This narrow-band whistling effect is called "sympathetic string resonance" or "resonance" herein. The wide-band sound halo effect is called "sympathetic string reverberation" or "reverberation" herein. Resonance seems favored by two main factors, tuning of strings and bridge mobility at the coupling point, according to the modal bases of the strings and bridge[8,9]. Frequency coincidence between a string partial and a body partial has been investigated by Gough[10] to tackle the wolf note problem that occurs in violin, viola, cello or double-bass. An unstable wolf note occurs when the string and body are strongly coupled at a specific frequency. The concept of frequency deviation, or veering, has been introduced when the eigenvalues of a vibratory system deviate after modes superimposition. This veering phenomenon is found in other vibratory systems in molecular physics, membrane or cable vibrations[11]. A coupling model of veering, in the case of a string mode and a body mode, has been studied by Woodhouse[12]. A veering phenomenon can explain double decay envelopes in coupled strings in a model with two degrees of freedom associated with the first modes of two different strings by

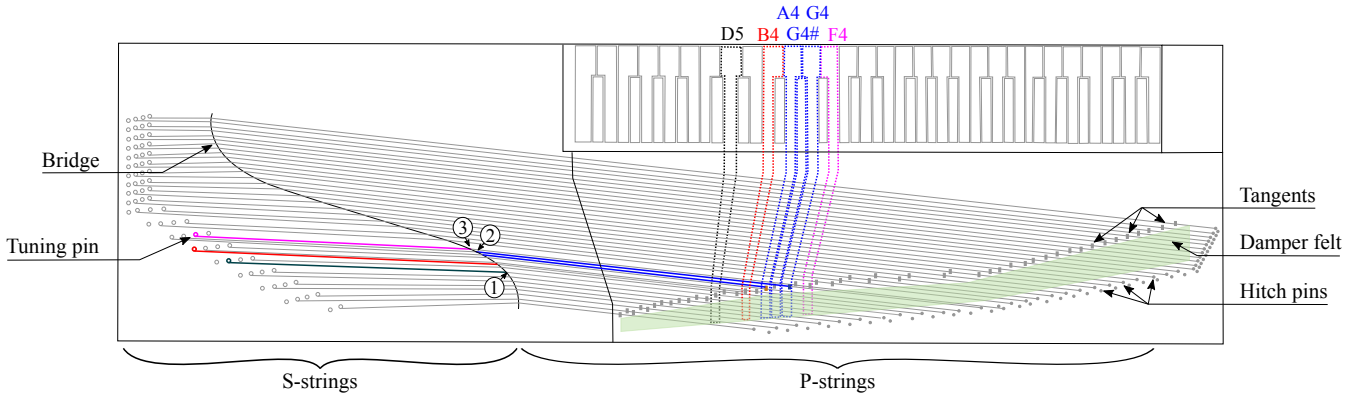

FIG. 1. Drawing of the clavichord model studied. P-strings are string segments between the tuning pin and the bridge, and S-strings are string segments between the bridge and the tangent. The five strings studied are colored: G#4/G4 and A4 P-strings in blue, meeting the bridge at point (2). B4 (resp. F4 and D5) S-string in red (resp. magenta and black) meeting the bridge close to point (2) (resp. at points (3) and (1)). The green band represents the damper felt inserted between tangents and hitch pins.

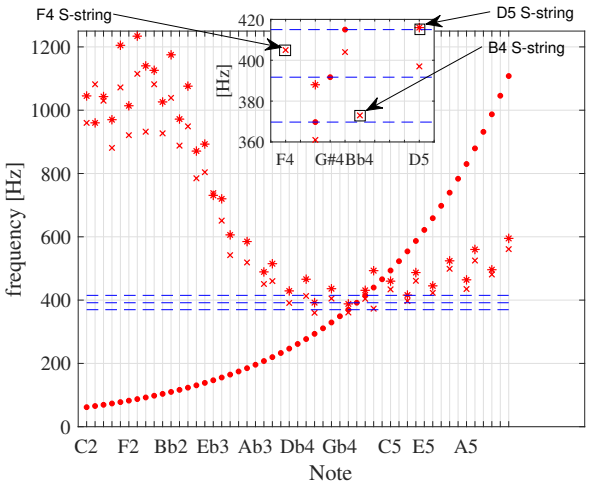

FIG. 2. Fundamental frequency (f_0) of the S-strings and P-strings. Circles represent f_0 of the P-strings; stars and a circle represent f_0 of a choir's first and second strings. Note that f_0 of the G4 key P-string and the B4 S-string are close together; f_0 of the G#4 key P-string and the F4 S-string are close together; f_0 of the A4 key P-string and the D5 S-string are close together. G4 and G#4 keys share the same P-string choir in this fretted clavichord model.

Weinreich[13]. Double-decay envelopes in stringed instruments have recently been revisited and extended, with another coupling formulation by Woodhouse[14]. Sympathetic string resonance is not specific to the clavichord. It is exploited for sound reinforcement in the duplex scale of the modern piano, e.g. Steinway & Sons[1]. Additional resonant strings, called "aliquot strings", are also found in Blüthner grand pianos.

This research aims to study S-strings resonance in the clavichord and the conditions driving the appearance of a whistling note. The hypotheses are that resonance depends on string modes' coincidence and interaction, that is, S-strings and P-strings tuning and bridge coupling mobility. The effects of tuning and coupling are investigated using experimental measurements and numerical simulation. Experiments are described in section II. After analyzing possible P-strings and S-strings f_0 (f_0) coincidences, three string candidates (keys G4, G#4 and A4) are selected. Bridge mobilities and S-string response to an excited P-string are measured and analyzed under different tuning configurations near resonance. Numerical resonance simulation, allowing for frequency veering analysis, is proposed in section III with the help of a reduced model of the studied clavichord. After estimating the bridge and string modal properties, a model based on the Udwadia-Kalaba (U-K) formulation is developed and implemented. Simulation and measurements are then compared. Section IV summarizes the results obtained and discusses the consequences of string resonance on the clavichord tonal quality and instrument design.

II. EXPERIMENTAL STUDY

This section selects three P-string and S-string pairs, contrasting in frequency, position and bridge mobility. Tuning of the S-strings is varied in the vicinity of the P-string f_0 to highlight the resonance effects. Finally, measurements of bridge mobility, bridge coupling and vibratory signals and subsequent analyses are performed and discussed.

A. Clavichord model and string frequency distribution

An instrument built in 2007 under the guidance of M. Ducornet by C. d'Alessandro and C. Besnainou at

The Paris Workshop (Montreuil, France) is studied. It is designed (by E. Dancet and M. Ducornet) according to German fretted models by Hubert (*ca* 1784, see the authoritative book by Brauchli for information on the clavichord[15]). The instrument encompasses 51 keys (C2-D6). It is double strung in brass, fretted by two above F3, resulting in 37 choirs, i.e. 74 strings arranged in pairs. Its dimensions are (mm) 1267×358×112. It is tuned using Kirnberger II temperament, with A4=415 Hz. The fundamental frequency (f_0) distribution for the 74 S-strings and P-strings are reported in Figure 2. When the two P-strings in a pair are tuned in unison, the corresponding two S-strings are not tuned in unison because their lengths are different between the bridge and the tuning pin. The 51 notes corresponding to the 74 P-strings have f_0 ranging from 62 Hz (key C2) and 1109 Hz (key D6), and the 74 S-string f_0 are distributed between about 380 Hz and 1200 Hz. The string frequency diagram of the instrument in Figure 2 shows several possible coincidences, and then possible resonances, between P-strings and S-strings f_0. As for the first transverse mode, resonance may occur for strings with similar lengths, diameters and tensions, the string material being the same brass for all strings. For f_0 and lengths, this region encompasses all P-strings above 350 Hz. However, if similar string diameters and tension are searched for, the region between 350Hz and 550 Hz (P-strings between keys G4 and D5) is the region of choice. In this region, P-strings and S-strings with similar lengths are also close on the bridge. Therefore, three P-string and S-string pairs are chosen for this study: G4(1) and B4(2), G#3(1) and F4(2), A4(2) and D5(1) ((1) and (2) indicate the first or second string in the choir). A drawing of the instruments showing the positions of these strings is displayed in Figure 1.

B. Tuning conditions

The P-string are tuned f_0 using an electronic tuner (Korg OT 12). Then f_0 of the S-string is varied around f_0 of the P-string in several steps using the electronic tuner. Variation of f_0 during a tone is a specific feature of the clavichord[16]. Then f_0 is measured after 0.5 s, after the attack transient. All the strings except the strings tuned are muted using strips of felt. The keyboard plays the P-string, and all the other strings, including the corresponding S-string are muted. The S-string is excited using a plectrum, all the other strings including the corresponding P-string are muted. For all string pairs, the S-string is tuned in 9 to 12 steps between -50 cents and +50 cents around resonance using the electronic tuner. The actual f_0 values obtained are then measured using Pitch Detection Algorithms (PDA) Yin and Praat (values automatically estimated with Yin[34] have been manually checked using Praat[35]). The precision obtained for $f0$ estimation procedures is limited to about 0.5 Hz (2 cents in the f_0 region of interest around 400 Hz), because of perceptual limits (the frequency difference limens[33] for pure tones is about 1 Hz or 4 cents at 440 Hz) and of the intrinsic f_0 variations of clavichord tones. All the values obtained are reported in Table I, with the corresponding number of steps.

C. Vibratory measurement methodology

The clavichord is installed in an acoustic studio with controlled temperature and humidity conditions because mechanical and vibratory properties of the clavichord soundboard are susceptible to temperature and humidity[20]. After preliminary experiments and tests of the set-up, the measurements are performed in three sessions. Frequency Response Function (FRF) measurements for the three sessions are checked to guarantee similar vibratory properties across sessions. Measurements, including soundboard and string responses, are repeated 2 to 5 times for each tuning condition.

Three string excitation conditions are measured: P-string alone, S-string alone, P-string and S-string in interaction. The string is excited by the tangent played by the key for the P-string alone and interaction conditions. The key is played with the help of the robotized finger DROPIC[17–19] that allows for repeatable string excitation. All the other strings are muted for the P-string alone condition. All the strings are muted except the measured P-string and S-string for the interaction condition. The S-string is excited by a hand-held plectrum for the S-string alone measurements. This type of excitation is not exactly repeatable, but it does not matter for f_0 estimation. Stings responses are measured with the help of three accelerometers (PCB M352C65) laid out on the bridge as shown in Figure 1 at three positions: (1) the D5 S-string coupling point, (2) the G4/G#4/A4 P-strings coupling point and (3) the F4 S-string coupling point. The same accelerometer installed between the G4/G#4 and A4 bridge pins is used for keys G4, G#4 and A4.

Sound examples of measurements are given in sound examples 1-6 (Multimedia file MM1 to MM6). Sound example 1 (Multimedia file MM1) is acceleration recorded at point (2) when the P-string is played on the G4 key, and all S-strings are damped. Sound example 2 (Multimedia file MM2) is a recording of acceleration at point (2) when the P-string is played on the G4 key, and the S-strings B4 is tuned close to resonance with G4. The sound is slightly reinforced in sound example 2 compared to sound example 1, with weakly audible beats.

Sound example 3 (Multimedia file MM3) is a recording of acceleration at point (2) when the P-string is played on the G#4 key, and all S-strings are damped. Sound example Sound example 4 (Multimedia file MM4) is a recording of acceleration at point (2) when the P-string is played on the G#4 key, and the S-strings F4 is tuned close to resonance with G#4. The whistling effect of the S-string appears when sound example 4 is compared to sound example 3. The timbre is reinforced with a phasing effect in sound example 4, because P-string and S-string are not precisely in unison.

Sound example 5 (Multimedia file MM5) is a recording of acceleration at point (2) when the P-string is played on the A4 key, and all S-strings are damped.

String	Length (mm)	f_0 (Hz)
G4 P-string n^{o}1	335	371.3
B4 S-string n^{o}2	334	360.3 363.2 365.9 367.6 368.3 368.5 369.3 370.6 371.4 373.8 375.4 379.5
G#4 P-string n^{o}1	315	392.2
F4 S-string n^{o}2	311	382.0 384.4 386.4 389.1 392.8 395.3 396.5 399.1 402.0
A4 P-string n^{o}2	300	415.4
D5 S-string n^{o}1	301	404.4 408.5 411.0 412.0 413.0 413.0 416.6 417.5 417.9 419.6 423.0 427.0

TABLE I. String lengths and f_0 around resonance for the G4 (resp. G#4, A4) P-string, corresponding to the B4 (resp. F4, D5) S-strings estimated by PDA (see Sec. II B). All strings in brass, diameters 0.33 mm (F4,G4,A4,B4), 0.3 mm (D5).

Sound example 6 (Multimedia file MM6) is a recording of acceleration at point (2) when the P-string is played on the A4 key, and the S-strings D5 is tuned close to resonance with A4. The whistling effect appears in sound example 6 compared to sound example 5; the tone lasts longer, with beats, because P-string and S-string are not precisely in unison.

S-string responses are measured with the help of a laser vibrometer (Polytech PDV 100). The laser beam is focused in the center of the measured S-string, between the bridge and the tuning pin. In addition, a calibrated omnidirectional measurement microphone (DPA 4006) records sound pressure 300 mm above the center of the soundboard. Figure 3 gives a picture of this experimental setting. Five signals are recorded for each string measurement: 3 accelerometer signals (bridge acceleration), a vibrometer signal (string velocity) and an acoustic signal (sound pressure level).

D. Measurement of bridge coupling mobilities

For the soundboard impulse response measurements, an automatic impact hammer (PCB 086E80) is placed at the G4 string coupling point (2). All strings are damped for measuring the bridge motion only. The bridge responses to impacts at the driven point are measured with the help of the three accelerometers. Velocity is obtained by frequency domain integration of the accelerometer signal. An FRF, defined as the velocity divided by the force in the frequency domain (mobility or admittance), is computed for each coupling point. Figure 4 shows the measured FRF H_{21} (resp. H_{22}, H_{23}) at the D5 (resp. F4, G4) coupling point. The three FRFs show only minimal magnitude and phase differences because of the different positions of the three accelerometers. The magnitudes of the three FRFs show a steep positive slope in our region of interest, between 350 and 420 Hz. The studied keys are chosen to exhibit the maximum mobility variation. The A4 P-string is located at a mobility peak near 420 Hz, the G4 P-string is located at a mobility valley near 360 Hz and the G#4 P-string is located just in between, around 392 Hz.

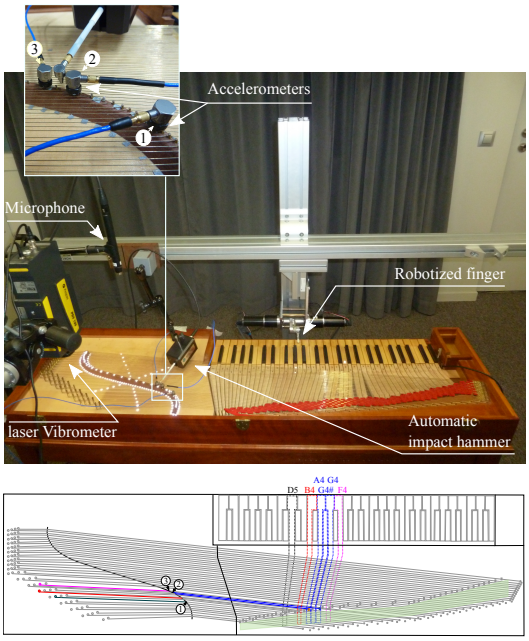

FIG. 3. Experimental set-up for measurements. A robotized finger plays the instrument. An automatic impact hammer is used for soundboard/bridge impulse response measurements. Velocity, acceleration, and sound pressure are measured by a laser vibrometer, three accelerometers and a microphone.

E. Velocity of the S-strings for different tuning and mobility conditions

Velocity signals measured at the center of the S-string for each tuning condition are presented in Figure 5. The signals represent the F-string oscillograms elicited by excitation of the P-strings, represented at f_0 positions in Table I. Vibratory amplitudes increase significantly when S-string and P-string frequencies are close, as expected for resonance. Amplitude modulations, or beats, result from mistuning between S-strings and P-strings. The more significant the frequency difference, the higher the beats frequency. Beats slow down, and the vibratory am-

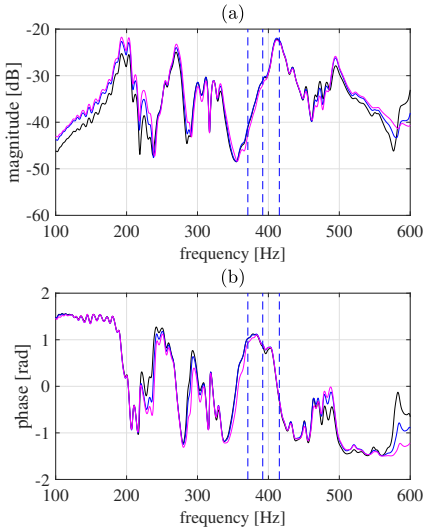

FIG. 4. Magnitude (a) and phase (b) of FRFs H_{21} (black), H_{23} (magenta), and H_{22} (blue). Vertical blue dashed lines show f_0 of G4, G#4 and A4 P-string. Ref 1 dB: 1 m.s^{-1}.N^{-1}.

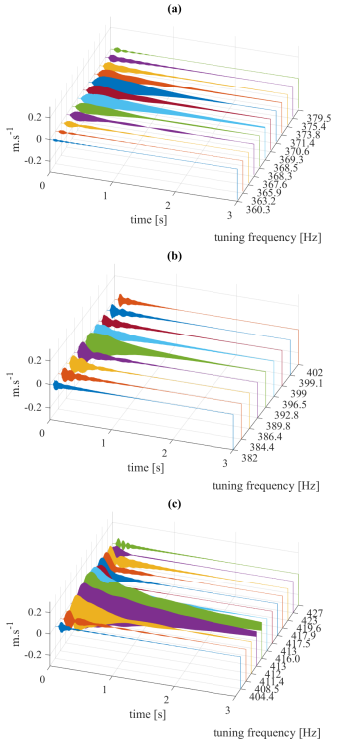

FIG. 5. Panel (a) (resp. b, c): string velocity in the middle of the S-string of the B4 (resp. F4, D5) S-string. The different oscillograms are for the different tuning conditions in Table I.

plitude increases When the frequency difference between the P-string and S-string decreases.

This result is consistent with previous results on string resonance[10] showing that frequency coincidence is a condition for resonance in the bridge mobility: a perturbation at the S-string coupling point leads to increased vibratory amplitude. Resonance depends on the bridge mobility, as shown by differences in amplitude response between the three pairs of strings. The S-string's amplitude response increases with a P-string's mobility at its coupling point on the bridge. Resonance is larger for A4 than for G#4 and for G#4 than for G4: resonance amplitude depends on frequency coincidence and mobility at the coupling point.

The root-mean-square (RMS) values of the velocity signals (integrated for 1 s) are displayed in Figure 6 for the different tuning conditions. The triangular shape of the figure indicates that the velocity increases when the S-string frequency comes closer to the P-string frequency. The RMS velocity is higher for the notes with higher mobilities. Despite all our effort, an exact f_0 coincidence of the P-string and S-string is never precisely reached. This deviation in f_0, possibly due to frequency veering at string resonance, is further investigated above.

F. Bridge coupling points acceleration for different tuning and mobility conditions

The RMS acceleration $a_{22,RMS}$ (integrated for 1 s) measured by the accelerometer at the G4/G#4 and A4 coupling point (2) is displayed in Figure 6, for the different tuning conditions. The signal captures the motions of both string segments in interaction. RMS acceleration is higher for the tones with higher mobilities, as expected. Almost no variation of RMS acceleration with tuning is observed within the accuracy of the error bars because the P-string dominates over the S-string in the acceleration signal.

G. String's fundamental mode estimation

f_0 detection is insufficient to investigate possible mode veering due to resonance. The acceleration signal measured at point (2) on the bridge contains contributions of the P-string and S-string horizontal and vertical vibration modes. A high-resolution modal estimation method is needed to disentangle these different modes. All the decreasing exponential components in the vicinity of f_0 the P-string excitation are identified using the ESPRIT high-resolution algorithm[9,21]. The analyses start 0.5 s after excitation to eliminate the effects of the attack transient and last for 2 s before the vibration vanishes. The signal is filtered by a Finite Impulse Response filter centered at the P-string f_0. Finally, the filter transient, corresponding to the first samples of the signal, is brushed aside from the ESPRIT analysis and signals are decimated to reduce computation time.

The estimated first mode frequencies for P-strings and S-strings are reported in Table II. Differences in Table I and II are minor despite theoretical differences between PDA estimation (assuming non-parametric adaptive f_0 estimation) and ESPRIT estimation (assuming time-invariant parametric estimation). These differences may reflect the different measurement conditions: strings

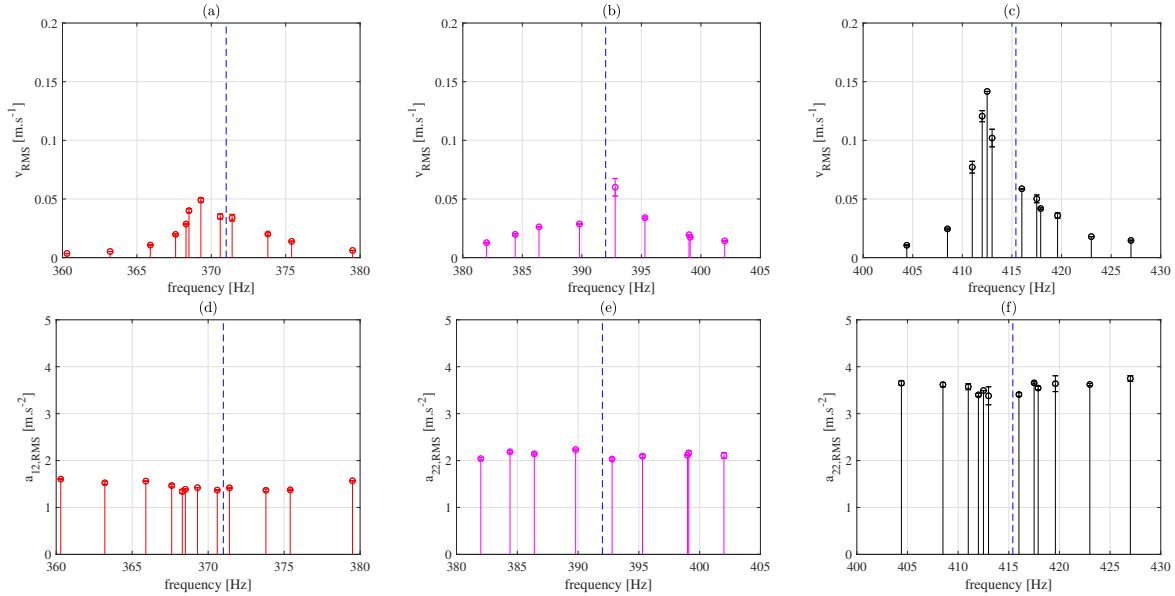

FIG. 6. RMS Velocity of the B4 (a), F4 (b) and D5 (c) S-string and RMS acceleration at point (2) on the bridge when playing the G4 (d), G#4 (e) and A4 (f) key, for f_0 in Table I.

are measured in interaction for Table II when measured separately for Table I. Again, an exact f_0 coincidence of the P-string and S-string is never reached, possibly due to frequency veering at string resonance. The modes frequencies and damping expressed in terms of the Exponential Sinusoidal Model used in ESPRIT are displayed in Figure 8 and discussed in the next section regarding simulation data.

III. SIMULATION STUDY

The veering phenomenon at resonance is difficult to observe and to demonstrate with the experimental data only, because of the limited number of experimental points and of the limited precision for f_0 estimation. Numerical simulation is proposed to overcome these limitations. Time-domain simulation of the string motion in a recently proposed model of the clavichord shows energy transmission from the P-string to the S-string (see the video example in[22]). In this section a reduced clavichord model using the Udwadia-Kalaba (U-K) formalism is developed. Following previous work[22], the model is reduced to the two P-strings and three S-strings. The simulated and measured data are compared to study mode veering at resonance.

A. Reduced clavichord model

A reduced clavichord model with five strings coupled to a bridge is considered to simulate the effect of bridge mobility on string resonance. The model is displayed in Figure 1, with three P-strings and three S-strings coupled to the bridge at point (1) (2) and (3). P-strings are set into vibration by the tangent, that is also one extremity (nut) of the string, according to the clavichord's mechanism. The tangent is modeled by a rigid body mode which becomes coupled with the string at the moment of contact[22]. The clavichord string is divided into three parts: The damped part is bounded by the hitchpin and the tangent, where a cloth strip is coiled up. The played part (P-string) is bounded by the tangent and the bridge coupling point. The sympathetic part (S-string) is bounded by the bridge coupling point and the tuning pin. Dampers coupled to the damped part of the clavichord strings are modeling the cloth strip damper of the real instrument. The bridge is modeled by means of the three coupling points considered.

B. The Udwadia-Kalaba formulation

In this section, the clavichord model in terms of coupled vibratory subsystems is modeled using a modal U-K formulation[23,24], a formalism that has been successfully used to date for physical modeling of the guitar, Portuguese guitar and clavichord[22,25,26]. Let us consider a mechanical system with mass matrix $\mathbf{M}$ which is subjected to a force vector $\mathbf{F_e}(t)$ including all constraint-independent internal and external forces. This system is also subjected to constraining forces $\mathbf{F_c}(t)$. Denoting the dynamical solution $\mathbf{y_u}(t)$ of the unconstrained system and $\mathbf{y}(t)$ of the constrained system, the motion equations of the constrained system derived by Udwadia and Kalaba[23,27] are:

$$\ddot{\mathbf{y}} = \ddot{\mathbf{y}}_u + \mathbf{M}^{-1/2}\mathbf{B}^{+}(\mathbf{b} - \mathbf{A}\ddot{\mathbf{y}}_\mathbf{u}), \quad \ddot{\mathbf{y}}_u = \mathbf{M}^{-1}\mathbf{F}_e(t) \quad (1)$$

where $\mathbf{A}$ is the constraint matrix and $\mathbf{b}$ the constrained vector obtained from the holonomic and (eventu-

String	f_0 (Hz)
G4 P-string n^{o}1	369.35 369.61 369.50 369.49 369.38 369.30 370.79 369.47 369.42 369.24 369.54 369.83
B4 S-string n^{o}2	360.06 363.44 366.23 368.01 368.86 369.53 370.79 370.97 371.68 374.30 376.71 379.93
G#4 P-string n^{o}1	392.57 393.01 392.75 392.96 392.36 393.56 392.43 392.48 392.51
F4 S-string n^{o}2	381.79 384.15 386.11 389.94 393.25 396.43 398.52 399.38 401.85
A4 P-string n^{o}2	416.24 416.44 416.46 416.80 416.46 416.48 415.89 415.41 415.73 415.62 415.90 415.75
D5 S-string n^{o}1	404.63 408.56 412.66 413.64 414.07 414.68 417.29 419.12 419.36 421.03 423.11 427.84

TABLE II. f_0 around resonance for the G4, G#4 and A4 P-string, and for the B4, F4 and D5 S-strings estimated by the high resolution ESPRIT algorithm (see Sec. III C).

ally) non-holonomic constraints, ϕ_p and ψ_p respectively, defined as:

$$\phi_p(\mathbf{y}, t) = 0, \quad p = 1, 2, \ldots, P_h \tag{2}$$

$$\psi_p(\mathbf{y}, \dot{\mathbf{y}}, t) = 0, \qquad p = P_h + 1, P_h + 2, \ldots, P_h + P_{nh} \tag{3}$$

where P_h and P_{nh} are the number of holonomic constraints and that of non-holonomic constraints respectively. By time differentiation of equation 2 and 4, it leads to the matrix-vector constraint equation in terms of accelerations:

$$\mathbf{A}(\mathbf{y}, \dot{\mathbf{y}}, t)\ddot{\mathbf{y}} = \mathbf{b}(\mathbf{y}, \dot{\mathbf{y}}, t) \tag{4}$$

The generalized Moore-Penrose inverse matrix $\mathbf{B}^+$ of $\mathbf{B} = \mathbf{A}\mathbf{M}^{1/2}$ can be rendered numerically robust, even for a singular constraint matrix. For a particular external excitation $\mathbf{F}_e(t)$ these equations are solved using a suitable time-step integration scheme. A modal version of the U-K formulation suitable for continuous flexible systems proved successful for musical instruments modeling[23]. Assuming a set of vibrating subsystems defined in terms of their unconstrained modal basis and coupled through kinematic constraints, one obtains[23]:

$$\ddot{\mathbf{q}} = \boldsymbol{W}\tilde{\mathbf{M}}^{-1}(-\tilde{\mathbf{C}}\dot{\mathbf{q}} - \tilde{\mathbf{K}}\mathbf{q} + \mathbf{F}_{\mathbf{ext}}) \tag{5}$$

where $\mathbf{q}$ represents the vector of modal displacements, $\tilde{\mathbf{M}}$, $\tilde{\mathbf{K}}$, $\tilde{\mathbf{C}}$ are respectively the modal mass matrix, modal stiffness matrix, and modal damping matrix, while $\boldsymbol{W} = \mathbf{1} - \tilde{\mathbf{M}}^{-1/2}\boldsymbol{B}^+\boldsymbol{A}$ is a convenient global transformation matrix (which is computed before the time loop), where $\boldsymbol{A}$ is the modal constraint matrix, and $\mathbf{F}_{\mathbf{ext}}$ are the external modal forces applied on the system.

C. Bridge modal parameter extraction

Modal analysis of the measured bridge FRF is used to extract the bridge modal parameters needed for simulation of the model. Physical poles containing the modal frequencies and damping coefficients of the analyzed structure are extracted using the least square rational function (LSRF) estimation method (Matlab signal processing toolbox[28]). Then, residues that encapsulate the mode shapes and modal masses of the system are estimated (normalizing modal masses to 1 kg).

Experimental modal analysis gives 47 bridge modes between 100 and 600 Hz. Accurate reconstruction of the FRF at the G4 P-string coupling point (point (2)) is al-

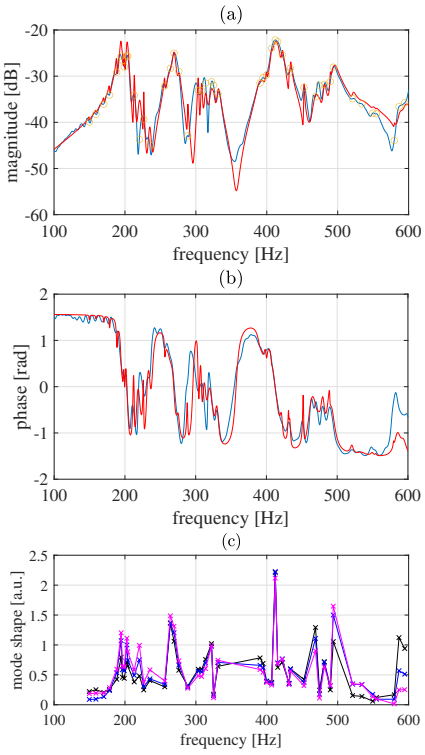

FIG. 7. Magnitude (a) and phase (b) of the measured (blue) and reconstructed (red) FRF with modal analysis at point (2), Ref 1 dB: 1 m.s^{-1}.N^{-1}. Mode shapes extracted out of this modal analysis at points (1) (red cross), (2) (blue cross) and (3) (magenta cross).

lowed with these modal parameters, as shown in Figure 7. The poles, modal masses and mode shapes of the system at point (1), (2) and (3) are derived for the sake of simulation[22].

D. Frequency and damping of coupled partials: experimental data and simulated data

Time domain simulations of the P-string and S-string motions are computed using the reduced clavichord model for all the experimental conditions in Table I. For each condition, frequency and damping of the P-string and S-string at the bridge are estimated for the simulation signals using the same high resolution ESPRIT method than for the experimental signals.

String modal parameters for the simulation are shown in Figure 8 for the 2 P-strings and the 3 S-strings studied using colored circles. Results are presented in the same way as Weinreich[13], with the centered frequency on the Y-axis (defined as the string frequency of the coupled system minus the tuned frequency, both for P-string or S-String) as a function of the mistuning between the P-string and the S-string frequencies ($\epsilon = f - f_0$, where f is the S-string frequency and f_0 the P-string frequency). The effect of bridge mobility on string resonance appears clearly on simulated data. Modal parameters of the P-string and S-string show frequency veering at resonance, and veering is higher in the case of higher mobility. The interaction between P-string and S-string is almost unnoticeable in the case of the G4 string, it appears for the G#4 string and it is clearly visible for the A4 string. The magnitude of frequency veering is modest (about 1-2 Hz) even in the largest case. Resonance also affects modal damping, with higher damping variation for higher resonance, i.e. higher mobility and smaller mistuning.

Measured data in Table II are superimposed to simulated data in Figure 8. Remember that experimental data are relatively scarce near resonance. Only two experimental points for A4 are actually close to resonance (near (0,0) in Figure 8, panel (c)). Frequency veering appears for this point. Both simulation and measurements show similar trends towards larger damping when bridge mobility increases and mistuning decreases.

In simulated as in experimental data when the tuning frequency of the S-string approaches P-string frequency from below, the S-string tends to increase when the P-string tends to decrease. Once the S-string frequency becomes larger than that of the P-string, the P-string tends to decrease when the S-string tends to increase. It is as though the frequencies of the two strings were exchanged.

The results obtained for damping are consistent with published data (see[14], Figure 8b), with the same order of magnitude for the Q-factors and the same bell-shaped response near resonance. The results are less accurate for experimental damping.

IV. SUMMARY AND CONCLUSION

A. Conditions for resonance

The conditions for S-string resonance, resulting in possible whistling tones, have been investigated in terms of frequency coincidence and bridge mobility. Possible frequency coincidences between P-strings and S-strings are consequences of the instrument design. Figure 2 shows that the region of 350-600 Hz contains the highest density of possible coincidence between P-strings and S-strings for our instrument. Three P-strings have been chosen G4, G#4 and A4, because of their almost perfect correspondence in length and f_0, with S-strings B4, F4 and D5.

The experiments indicate that fine-tuning is the first condition for whistling tones to appear. Figure 5 shows the amplitude of S-string responses as a function of tuning accuracy, varied in 9 to 13 steps around the resonance frequency. The amplitude response is maximum close to f_0 coincidence. Coupling mobilities between P-strings and F-strings are estimated through impulse response and FRF measurements on the bridge. The bridge mobility is larger for A4 than for G#4 and for G#4 than for G4, as shown on the FRF (Figure 4), leading to a larger vibratory amplitude for A4 than for G#4 and for G#4 than for G4 (Figure 6). Then, higher mobility is a second condition for higher resonance.

B. Effect of resonance

When a P-string partial frequency coincides with the S-string partial, the S-string resonates. At resonance, a veering of the S-string partial frequency and damping is observed[29], because of the bridge motion at the coupling point. The force exerted on the bridge by the P-string and S-string moving together at the same frequency is responsible for this specific bridge motion. It leads to a change in the S-string effective length and the S-string energy loss to the soundboard, and hence a shift of the S-string partial frequency and damping[13]. The larger this bridge motion, the larger the string's effective length and energy loss. In that situation, the veering of the coupled sympathetic string partial frequency and damping becomes larger.

In the case of the studied clavichord, it has been shown (Figure 8) that higher mobility P-strings present more significant shifts in frequency and damping at resonance. This difference in veering is observed experimentally and verified through simulated data based on the Udwadia-Kalaba formulation. Weinreich first demonstrated this tendency in the case of two identical strings coupled to the same coupling point[13]. Weinreich's model shows that the shift in frequency and damping of the coupled strings at frequency coincidence is proportional to the bridge mobility. The same effect is shown in our simulated data. The Udwadia-Kalaba formulation and the Weinreich model give equivalent results for the P-string and S-string coupling situation[30].

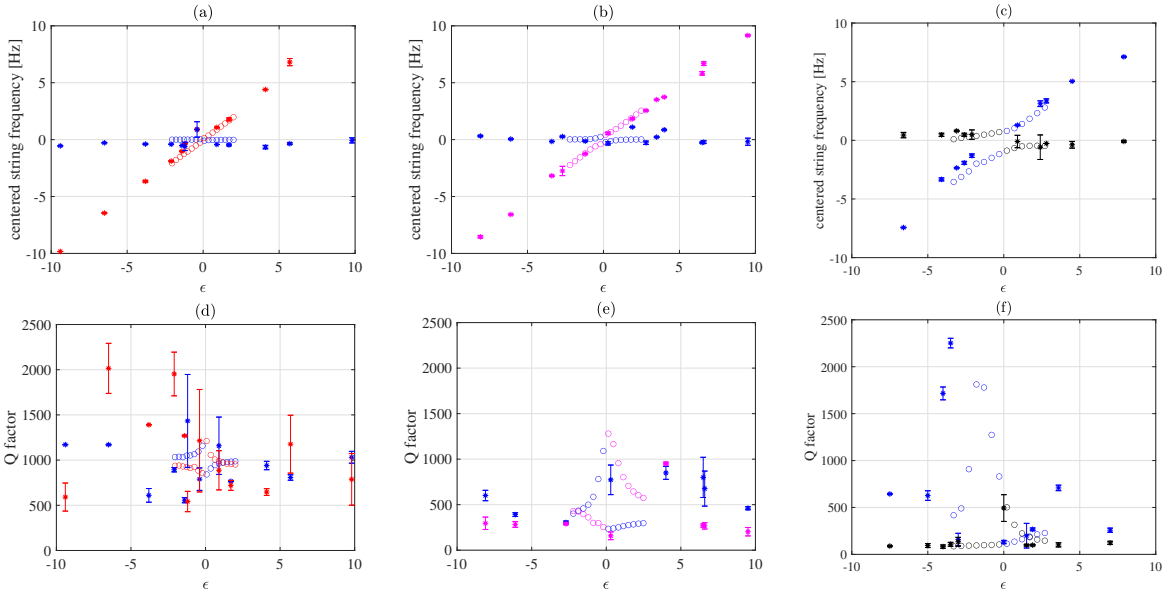

FIG. 8. Centered frequency and damping as functions of mistuning for G4 (a,d), G#4 (b,e) and A4 (c,f) P-strings in blue and B4 (a,d in red), F4 (b,e in magenta) and D5 (c,f in black) S-strings. Stars represent experimental data (with standard deviation for five repetitions), and circles represent simulated data.

C. Whistling and consequences of sympathetic resonance in the clavichord

Under some conditions, sympathetic resonance in the clavichord can cause a significant amplitude response of an S-string, resulting in a distinctive or whistling tone. However, too loud a whistling is considered undesirable for musical performance because it can undermine the instrument's timbre homogeneity and power equality.

It has been remarked by clavichord tuners that string coupling and resonance can impair fine-tuning adjustment: *"But there is a further refinement: it is possible for the string to be precisely in unison but to produce a sound that is dull, short-lived and 'dead'. [...] To make the note sing, you need to sharpen one of the two strings very, very slightly: not enough to cause perceptible wavering or beats."*[31]. The same effects have been observed in our study when a S-string is tuned in unison with a P-string : the increase of damping corresponds to a *sound that is dull, short-lived and 'dead'* and frequency veering made it difficult to tune the P-string and S-string to an exact stable unison (*one of the two strings is very, very slightly* detuned).

Sympathetic vibration depends much on the instrument design and stringing pattern. The widest instruments, e.g. German and Nordic XVIIIth century models, have long soundboards and S-strings and consequently long reverberation time and possibly loud whistling tones.

Sound examples 7-10 (Multimedia file MM7-MM10) are recorded on a copy of a large unfretted instrument by Friererici (Musée de la Musique, Paris) built in 2016 by Renée Geoffrion (Unacorda workshop, Pierre Buffière, France).

Sound example 7 (Multimedia file MM7) is the Sound Pressure Level (SPL) recorded above the soundboard when the first P-string F4 is played on the F4 key, and all S-strings are damped. Sound example 8 (Multimedia file MM8) is the SPL when the first P-string F4 is played on the F4 key, the second S-strings F4 being tuned close to resonance with F4. The length of the first P-string and the second S-string of the choir for this particular key are equal. String are contiguous on the soundboard and belong to the same choir of strings. Short notes are played for both examples. The effect of the S-string is a loud sympathetic whistling lasting after the F4 key has been released.

Sound example 9 (Multimedia file MM9) is the SPL recorded the soundboard when the second P-string A4 is played on the A4 key, and all S-strings are damped. Sound example 10 (Multimedia file MM10) is the SPL when the second P-string A4 is played, the first S-strings B4 being tuned close to resonance with A4. String are contiguous on the soundboard but belong to two different choirs of strings. Short notes are played for both examples. The effect of the S-string is a loud sympathetic whistling lasting after the A4 key has been released.

A systematic study of instrument design regarding its consequences on reverberation would be interesting for clavichord makers or historically informed practice. Frequency coincidence between strings partials is highly praised in the concert harp or the duplex scale of the piano for its effect on the radiated sound. Therefore, the model of sympathetic strings and soundboard dynamics

developed in this article could be helpful for these instruments.

[1]Fredrik Öberg and Anders Askenfelt, Acoustical and perceptual influence of duplex stringing in grand pianos. The Journal of the Acoustical Society of America, 131 (1), P. 856-871, 2012.

[2]Sebastian Virdung. *Musica Getutscht*. Bâle, 1511.

[3]Marin Mersenne. *Harmonie universelle, contenant la thèorie et la pratique*. Sébastien Cramoisy, Paris, 1636.

[4]Jakob Adlung. *Musica mechanica organoedi: Das ist: Gründlicher Unterricht von der Struktur, Gebrauch und Erhaltung, &c. der Orgeln, Clavicymbel, Clavichordien und anderer Instrumente, in so fern einem Organisten von solchen Sachen etwas zu wissen nöhtig ist*, volume 1. FW Birnstiel, 1768.

[5]Christophe d'Alessandro and Brian F.G. Katz. Tonal quality of the clavichord: The effect of sympathetic strings. In *Proceedings of the International Symposium on Musical Acoustics ISMA '04*, pages 21–24, 2004.

[6]Jean-Théo Jiolat. *Vibro-acoustic study of the clavichord*. PhD thesis, Sorbonne université, 2021.

[7]Jean-Théo Jiolat, Jean-Loic Le Carrou and Christophe d'Alessandro. L'effet acoustique des cordes mortes du clavicorde. In *Congrès Français d'Acoustique, CFA 2018*, pages 233–239, 2018.

[8]Jean-Loïc Le Carrou, Francois Gautier, Nicolas Dauchez, and Joël Gilbert. Modelling of sympathetic string vibrations. *Acta Acustica united with Acustica*, 91(2):277–288, 2005.

[9]Jean-Loïc Le Carrou, François Gautier, and Roland Badeau. Sympathetic string modes in the concert harp. *Acta Acustica united with Acustica*, 95(4):744–752, 2009.

[10]Colin E. Gough. The theory of string resonances on musical instruments. *Acta Acustica united with Acustica*, 49(2):124–141, 1981.

[11]N.C. Perkins and C.D. Mote Jr. Comments on curve veering in eigenvalue problems. *Journal of Sound and Vibration*, 106(3):451–463, 1986.

[12]Jim Woodhouse. On the synthesis of guitar plucks. *Acta Acustica united with Acustica*, 90(5):928–944, 2004.

[13]Gabriel Weinreich. Coupled piano strings. *The Journal of the Acoustical Society of America*, 62(6):1474–1484, 1977.

[14]Jim Woodhouse. A necessary condition for double-decay envelopes in stringed instruments. *The Journal of the Acoustical Society of America*, 150(6):4375–4384, 2021.

[15]Bernard Brauchli. *The clavichord*. Cambridge University Press, 1998.

[16]Christophe d'Alessandro. On the dynamics of the clavichord: From tangent motion to sound. *The Journal of the Acoustical Society of America*, 128 (4): 2173–2181, 2010.

[17]Alexandre Roy. *Développement d'une plate-forme robotisée pour l'étude des instruments de musique à cordes pincées*. PhD thesis, Paris 6, 2015.

[18]Jean-Loic Le Carrou, Delphine Chadefaux, Marie-Aude Vitrani, Sylvère Billout, and Laurent Quartier. Dropic: A tool for the study of string instruments in playing conditions. In *Acoustics 2012*, 2012.

[19]Delphine Chadefaux, Jean-Loic Le Carrou, Marie-Aude Vitrani, Sylvère Billout, and Laurent Quartier. Harp plucking robotic finger. In *2012 IEEE/RSJ International Conference on Intelligent Robots and Systems*, pages 4886–4891, Oct 2012.

[20]Daniel Konopka, Stefan Ehricht, and Michael Kaliske. Hygromechanical investigations of clavichord replica at cyclic climate load: experiments and simulations. *Journal of Cultural Heritage*, 36:210–221, 2019.

[21]Richard Roy and Thomas Kailath. Esprit-estimation of signal parameters via rotational invariance techniques. *IEEE Transactions on acoustics, speech, and signal processing*, 37(7):984–995, 1989.

[22]Jean-Théo Jiolat, Christophe d'Alessandro, Jean-Loïc Le Carrou, and Jose Antunes. Toward a physical model of the clavichord. *The Journal of the Acoustical Society of America*, 150(4):2350–2363, 2021.

[23]Jose Antunes and Vincent Debut. Dynamical computation of constrained flexible systems using a modal udwadia-kalaba formulation: Application to musical instruments. *The Journal of the Acoustical Society of America*, 141(2):764–778, 2017.

[24]Jose Antunes, Vincent Debut, Laurent Borsoi, Xavier Delaune, and Philippe Piteau. A modal udwadia-kalaba formulation for vibro-impact modelling of continuous flexible systems with intermittent contacts. *Procedia engineering*, 199:322–329, 2017.

[25]Vincent Debut, Jose Antunes, Miguel Marques, and Miguel Carvalho. Physics-based modeling techniques of a twelve-string portuguese guitar: A non-linear time-domain computational approach for the multiple-strings/bridge/soundboard coupled dynamics. *Applied Acoustics*, 108:3–18, 2016.

[26]Vincent Debut and Jose Antunes. Physical synthesis of six-string guitar plucks using the udwadia-kalaba modal formulation. *The Journal of the Acoustical Society of America*, 148(2):575–587, 2020.

[27]Ara Arabyan and Fei Wu. An improved formulation for constrained mechanical systems. *Multibody System Dynamics*, 2(1):49–69, 1998.

[28]Ahmet Arda Ozdemir and Suat Gumussoy. Transfer function estimation in system identification toolbox via vector fitting. *IFAC-PapersOnLine*, 50(1):6232–6237, 2017.

[29]Jim Woodhouse. Plucked guitar transients: Comparison of measurements and synthesis. *Acta Acustica united with Acustica*, 90(5):945–965, 2004.

[30]Jean-Théo Jiolat, Christophe d'Alessandro, and Jean-Loic Le Carrou. Vibrations par sympathie dans le clavicorde. In *Congrès Français d'Acoustique, CFA 2022*, 2022.

[31]Peter Bavington Clavichord Tuning and Maintenance (p. 12) Keyword Press, London, 2007.

[32]John Barnes Coupling between clavichord unisons ands its effect on tuning In *Het Clavichord, Year 2, No3*, Netherlands Clavichord Society 1989.

[33]E. G. Shower and R. Biddulph. Differential pitch sensitivity of the ear," J. Acoust. Soc. Am. 3, 275-287, 1931.

[34]Alain de Cheveigné and Hideki Kawahara. YIN, a f_0 estimator for speech and music. J. Acoust. Soc. Am. 111, 1917–1930, 2002.

[35]Praat: doing phonetics by computer [Computer program]. Version 6.3, retrieved 15 November 2022 from http://www.praat.org/ Paul Boersma and David Weenink. Praat: doing phonetics by computer [computer program]. Version 6.3, retrieved 15 November 2022 from http://www.praat.org/